

Effect of Off-Axis Concentrated Loading on Failure of Curved Brittle Layer Structures

Tarek Qasim,¹ Christopher Ford,¹ Mark B Bush,¹ Xiaozhi Hu,¹ Brian R. Lawn²

¹ School of Mechanical Engineering, The University of Western Australia, Crawley, W.A. 6009, Australia

² Materials Science and Engineering Laboratory, National Institute of Standards and Technology, Gaithersburg, Maryland 20899-8500

Received 21 December 2004; revised 8 April 2005; accepted 10 May 2005

Published online 29 August 2005 in Wiley InterScience (www.interscience.wiley.com). DOI: 10.1002/jbm.b.30373

Abstract: A study is made of the effects of superposed tangential force by off-axis indentation loading on curved bilayers consisting of brittle shells filled with polymer support material. Such loadings are pertinent to all-ceramic crown structures on tooth dentin in occlusal function. Layer flexure places the ceramic undersurfaces in tension, leading to fracture by initiation and propagation of radial cracks. Following an earlier study, model specimens with curved surfaces are prepared by pressing glass plates 1 mm thick onto steel spherical dies with radius of curvature 20 mm to 8 mm at elevated temperatures, and bonding the resultant hemispherical shells onto an epoxy support base. The specimens are tested by indentation with spheres loaded vertically but off-center, with the contact center located at 30° to the hemisphere axis. The applied loads to initiate radial cracks are little affected by the resultant tangential component, but the loads to propagate the same cracks to the specimen edges are substantially reduced. Finite element calculations are used to evaluate stress states in the specimens for correlation with the experimental data. © 2005 Wiley Periodicals, Inc.* J Biomed Mater Res Part B: Appl Biomater 76B: 334–339, 2006

Keywords: curved surfaces; radial cracks; contact damage; brittle layers; crown failure; tangential loading

INTRODUCTION

A recent study conducted in our laboratories describes the fracture of brittle layers bonded to curved polymeric support substrates from concentrated surface loading.¹ In that study, a hard spherical indenter was used to deliver central normal loads by aligning the loading system with the axis of symmetry of the hemispherically shaped specimen surfaces. Fracture occurred by radial cracking at the brittle layer undersurface, initially confined to the contact area but subsequently, at increased load intensity, accelerating to the curved specimen extremities. Normal loading configurations have formed the basis for most contact fracture testing of this kind, enabling the evaluation of relevant material properties and thicknesses with minimum complication.^{2–13}

Such fracture systems are of intense interest as a simulation of the occlusal failure of convoluted dental crowns and

other biomechanical systems. Whereas occlusal contact in dental systems is generally quite complex^{14–22}—involving, among other factors, chemical interactions with water, cumulative rate effects from repetitive loading, residual stresses in the ceramic components, presence of a third material during chewing—experiments on model curved layer systems nevertheless afford physical insight into basic damage modes. One complicating factor of special interest is the effect of off-axis loading: occlusal loading in dental function is generally far from normal and symmetrical, involving off-center tangential and even rotational elements. Any complete analysis of dental crown failure requires these elements to be incorporated into the description. Although one earlier investigation of superposed tangential loads on *flat* brittle layers has suggested a relatively minor effect in the critical conditions to *initiate* radial cracks,⁵ the question remains as to any effect of such superposed loads on ultimate failure.

This article aims to measure the effect of a superposed tangential component in the applied loading on the growth of radial cracks to failure in convex brittle layer specimens. As before,¹ borosilicate glass plates molded over steel sphere dies at elevated temperatures are used to produce hollow glass hemispherical shells, which are then pressed and bonded onto an epoxy resin base to produce filled bilayers

Correspondence to: B. R. Lawn (e-mail: brian.lawn@nist.gov)

Contract grant sponsor: Australian Research Council

Contract grant sponsor: Gledden Senior Fellowship at UWA

Contract grant sponsor: U.S. National Institute of Dental and Craniofacial Research; contract grant number: PO1 DE10976

© 2005 Wiley Periodicals, Inc. *This article is a US Government work and, as such, is in the public domain in the United States of America.

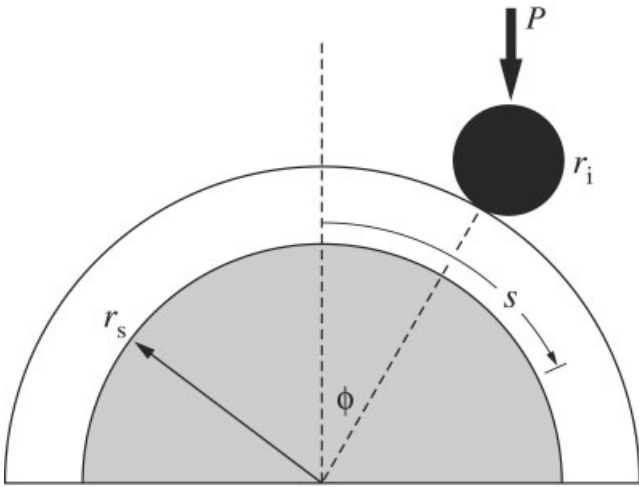


Figure 1. Loading of indenter of radius r_i at vertical load P on a convex curved brittle layer of inner radius r_s bonded to a compliant support base. Off-axis contact is made at angle ϕ to shell axis. Coordinate s measures circumferential distance along undersurface of brittle layer from specimen axis in a plane containing load axis.

with surfaces of specifiable inner radii. A hard sphere is used to apply a concentrated load to the specimen top surfaces, vertically applied but off-axis relative to the specimen center so that a tangential force is superposed onto the usual normal force. Radial crack evolution is followed *in situ* using a video camera system. It is confirmed that the superposed tangential load has a negligible effect on the critical loads to initiate subsurface radial cracks, but substantially diminishes the load to propagate those same cracks to ultimate failure.

EXPERIMENTAL PROCEDURE

As described in a preceding article, borosilicate glass shells were prepared by pressing slides 1 mm thick onto steel spherical dies with radius of curvature $r_s = 20$ mm to 8 mm at elevated temperatures.¹ The glass undersurfaces were given an abrasion treatment with 50 μm sand particles using a dental sandblast machine, in order to produce a uniform density of surface flaws for crack initiation and to reduce the strength of the glass to near that of porcelain.² (Tests on glass with unabraded surfaces, or on other stronger ceramics, simply shift the ensuing critical loads to higher levels without changing the general data trends.¹) The glass shells were then pressed into a mold containing epoxy resin, so filling the shell interior, with the convex glass surface facing outward and the abraded surface inward. The resulting specimen configuration is depicted schematically in Figure 1. To avoid residual stresses in the glass, the epoxy was applied in thin layers < 5 mm, allowing each successive layer to cure under the action of a slow hardener for 1 day before adding the next. Polished sections through the specimens revealed intimate bonding without any sign of delamination from the substrate. Small Vickers indentations placed in the polished glass sections (indent corner diagonals aligned parallel and perpendic-

ular to the layer surfaces) showed symmetrical crack patterns, confirming the absence of significant residual stresses (i.e., < 10 MPa).²³

Surface loading of the specimens was carried out in air using a tungsten carbide sphere of radius $r_i = 4$ mm (representative of dental cuspal radii)^{22,24} mounted in a screw-driven mechanical testing machine. Loads up to $P = 1500$ N were applied. The specimen was carefully located so that the load axis was off-center, corresponding to vertical loading at a contact point $\phi = 30^\circ$ to the axis of symmetry, with resultant normal component $P_n = P \cos 30^\circ = 0.87P$ and tangential component $P_t = P \sin 30^\circ = 0.50P$. Accordingly, the normal load on the surface was slightly reduced relative to axial loading, but now augmented by a substantial tangential component. The specimens were clamped to prevent any sliding during testing. A video camera was placed to view the fracture evolution during the loading cycle, with a light source to provide back illumination. A single-cycle indentation was performed at $\sim 10 \text{ N}\cdot\text{s}^{-1}$ on each specimen. Critical loads $P = P_R$ to initiate radial cracks at the glass undersurfaces were monitored. The critical events were detectable visually by the video camera, accompanied by audible clicks in some cases. In cases where visibility was limited, initiation was inferred from a load drop in the load-time record.²⁵ Subsequent failure loads $P = P_F$ were deemed to be attained when the cracks reached the hemispherical extremities of the specimen. Four to eight specimens were tested at each surface radius. No delamination was observed between the glass and epoxy in any of the tests until failure, confirming good bonding.

Similar to our preceding paper,¹ finite element modeling was used to compute hoop stresses (stresses normal to the plane of Figure 1) at the glass undersurfaces, except that provision was made for the essentially three-dimensional (3D) nature of the current configuration. Details of the FEA procedures, using Abaqus V6.4 software, have been well documented.^{13,26,27} We are concerned with the variation of the hoop stress as a function of curvilinear coordinate s along the brittle layer undersurface from the specimen center and contained in the plane of the contact and loading axis in Figure 1. As before, the lateral specimen dimensions were 8 mm \times 8 mm and the support thickness below the hemispherical base was 6 mm. Input Young's modulus and Poisson's ratio were 73 GPa and 0.21 for the glass, 3.4 GPa and 0.33 for the epoxy, and 614 GPa and 0.3 for the tungsten carbide indenter. Contact was assumed to be frictionless. The meshes were systematically refined, particularly in the critical glass undersurface region, until the solutions attained convergence. The mesh consisted of up to 223,540 3D elements, with a minimum element size 10 μm in the contact zone. As a further check on the reliability of the 3D code, intercomparison was made with an even higher mesh density 2D analysis of the special case of symmetrical on-axis loading configuration—agreement in stress values to within 1% was obtained.

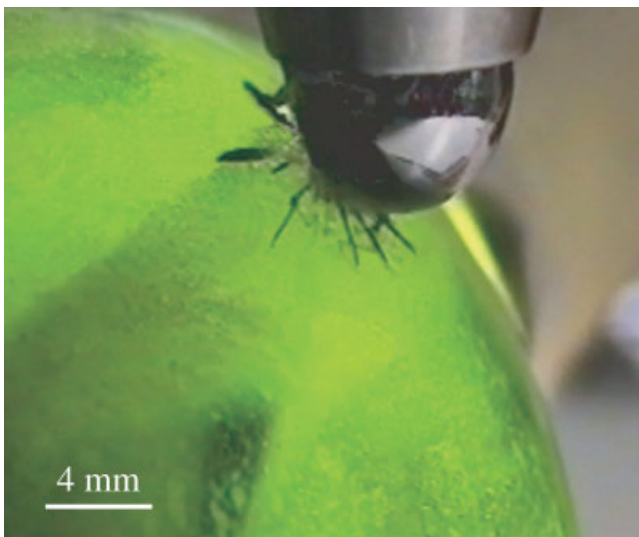


Figure 2. Radial cracks in convex glass layer of thickness 1 mm and inner radius $r_s = 20$ mm with abraded undersurface on epoxy resin substrate, from off-axis loading at $\phi = 30^\circ$ with WC sphere of radius $r_i = 4$ mm at load $P = 340$ N. Note symmetry of radial crack pattern relative to the specimen surface normal through the contact center.

RESULTS

Crack Morphology

Figure 2 shows a representative *in situ* photograph of off-axis contact loading ($\phi = 30^\circ$) using a WC sphere of radius $r_i = 4$ mm at $P = 340$ N on a curved glass/polycarbonate specimen of brittle-layer inner radius $r_s = 20$ mm. (For comparison, the critical load for radial crack initiation for this specimen geometry is $P_R \approx 125$ N.) The multiple cracks radiate symmetrically about the surface normal, a general observation for all radial crack patterns in their initial stages of growth, whether the loading be axial or off-axis. This result is in accord with earlier observations from tests with inclined-loading on flat specimens, confirming a minor role in the radial crack initiation.⁵

Figure 3 shows radial crack patterns at a later stage of evolution, at $P = 500$ N, comparing axial loading at $\phi = 0$ and off-axis loading at $\phi = 30^\circ$ for a specimen radius $r_s = 11$ mm. The key observation here is that the radial crack has propagated to the boundary of the hemispherical specimen in (b) but not in (a), suggesting that off-center loading is more likely to cause failure. The symmetry of the radial crack pattern tended to be broken in this region of well-developed radial cracks, with a pronounced tendency for the cracks to extend more rapidly and unstably toward the immediate specimen edges with increasing load. At higher loads, neighboring radial cracks began to link up at their base, dislodging triangular glass fragments. Some top-surface ring cracks were evident around the contacts at these higher loads, but always occurred after the radial cracks and therefore played a secondary role in the specimens examined here.

Quantitative Radial Crack Evolution

Figure 4 plots off-axis ($\phi = 30^\circ$) critical loads P_R to initiate subsurface radial cracks in the curved specimens with

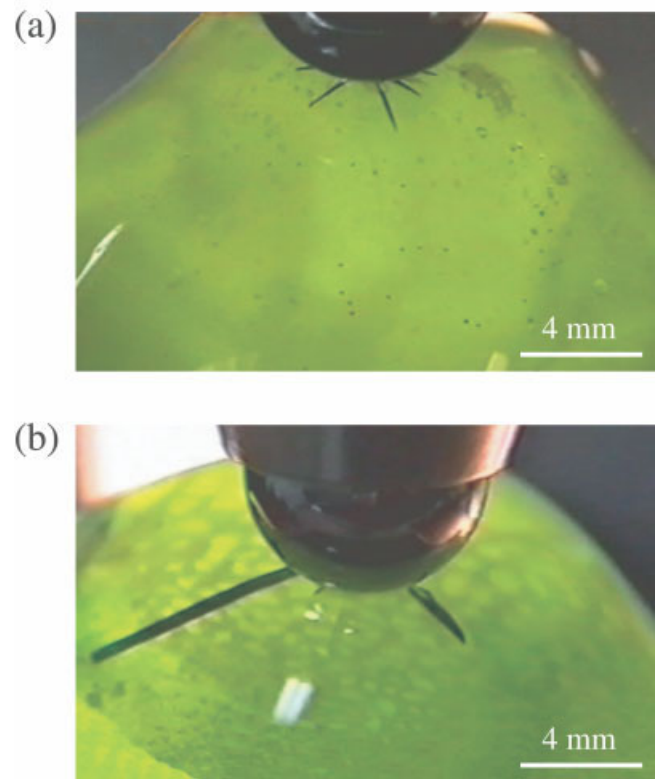


Figure 3. Radial cracks in convex glass layers of thickness 1 mm and inner radius $r_s = 11$ mm with abraded undersurface on epoxy resin substrate, from loading with WC sphere of radius $r_i = 4$ mm at load $P = 500$ N. (a) Axial loading, $\phi = 0$; (b) off-axis loading, $\phi = 30^\circ$.

abraded glass undersurfaces, as a function of specimen curvature r_s^{-1} . Each data point is a mean and standard deviation bound. Data for axial loading are included from our preced-

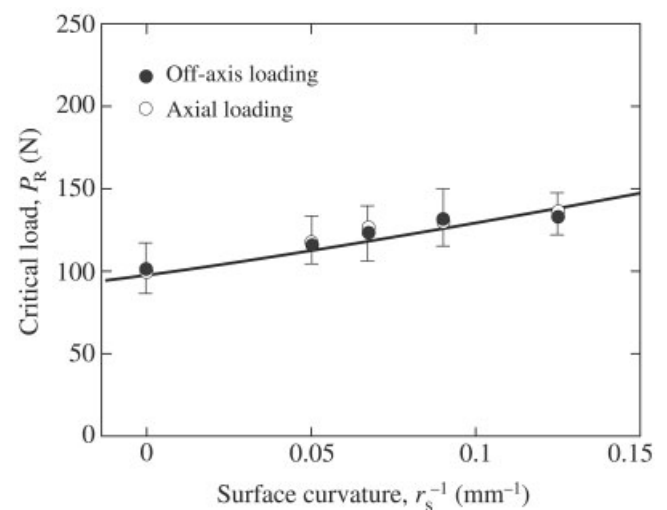


Figure 4. Critical load P_R to initiate radial cracks in convex glass layer of thickness 1 mm with abraded glass undersurfaces, as function of inverse surface radius r_s^{-1} . Loading with WC sphere of radius $r_i = 4$ mm. Data are means and standard deviations. Solid line is FEA computation.

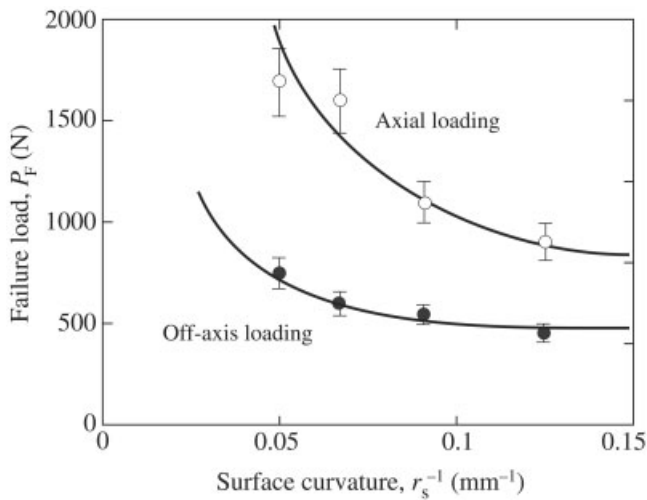


Figure 5. Failure loads P_F to propagate radial cracks to base of convex glass layers of thickness 1 mm with abraded undersurfaces, from loading with WC sphere of radius $r_i = 4$ mm, as function of inverse surface radius r_s^{-1} . Data are means and standard deviations. Solid curves are empirical spline fit.

ing study on normal loading ($\phi = 0$) for comparison.¹ The data for axial and off-axis loading overlap within the scatter bounds, indicating that the small reduction in normal loading ($P_n = 0.87P$) is inconsequential in the crack initiation, as is superposition of the tangential component ($P_t = 0.50P$). As before, solid lines are from FEA computations using a best-fit strength $S = 75$ MPa for abraded surfaces to determine the critical loads for crack initiation at the glass lower surfaces. The computations account for the principal data trends.

Figure 5 plots off-axis failure loads P_F to extend radial cracks around the hemispherical glass shells to the specimen boundaries, as a function of surface curvature. Data points are again means and standard deviations. Again, data for axial loading from our preceding study are included.¹ In this case the solid lines are empirical spline fits to the data. The two data sets now show very distinct differences, with the off-axis failure loads about a factor of two smaller than their axial counterparts.

To account for the reduction in failure load for off-axis loading, Figure 6 shows contours of hoop tensile stress below a vertically loaded contact for an indenter of $r_i = 8$ mm at $\phi = 30^\circ$ and $P = 200$ N, for a plane containing the specimen and loading axes. These stresses have the typical form for a plate flexing on a soft support, but here skewed because of the asymmetrical loading.^{2,28} As can be seen from Figures 4 and 5, 200 N is higher than the load needed to initiate radial cracks in this configuration, but considerably less than that to cause final failure. The contours remain relatively symmetrical in the immediate vicinity of the surface normal through the contact center, but elongate toward the near specimen boundary at larger circumferential distances. Figure 7 plots the tensile stresses at the glass undersurface for this same configuration as a function of circumferential coordinate s measured from the specimen symmetry axis (Figure 1). A

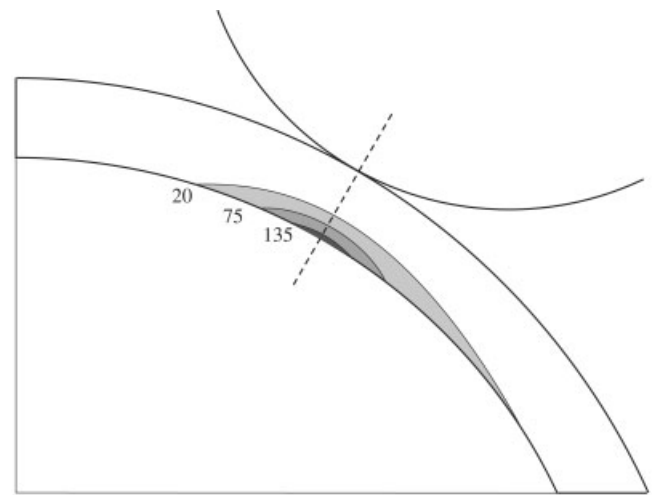


Figure 6. Contours of hoop tensile stress in glass layer of inner radius $r_s = 8$ mm on epoxy substrate, indicating plate flexure on compliant underlayer. Note asymmetry of long-range stress distribution. (Hertzian stresses omitted.)

comparative curve for axial loading from our preceding study is included.¹ The maxima in the curves for the two loading geometries are located immediately below the contact center along the surface normal, in accord with Figure 6. That for off-axis loading is slightly lower than for axial loading, consistent with the data in Figure 4 and commensurate with the slight reduction in normal load component ($P_n = 0.87P$). Note that the off-axis maximum of 150 MPa is about twice the strength of the glass, $S = 75$ MPa, indicated above. The stress distribution for the off-axis curve is slightly enhanced in the direction closer to the specimen edge, consistent with

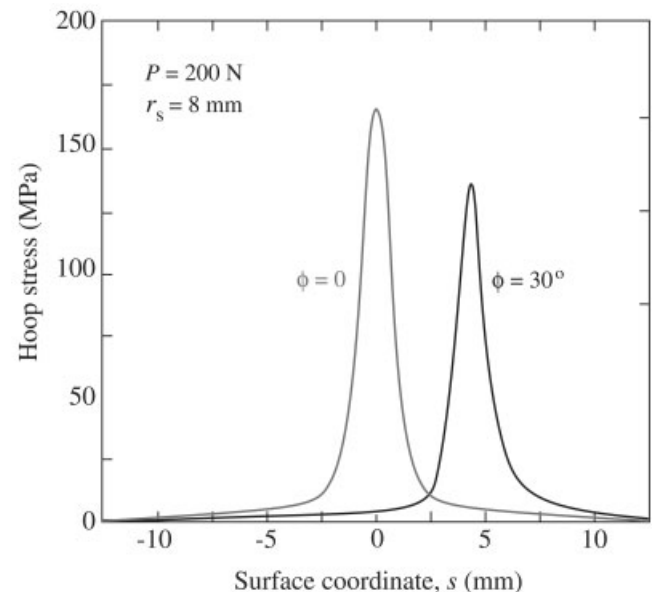


Figure 7. Plot of FEA-generated hoop tensile stress at undersurface of glass layer of inner radius $r_s = 8$ mm on epoxy substrate as a function of circumferential coordinate s . Comparing curves for axial ($\phi = 0$) and off-axis ($\phi = 30^\circ$) loading at $P = 200$ N.

the crack pattern asymmetry observed in Figure 3(b). Moreover, in this region the stresses are substantially higher than for the axial loading counterpart, accounting for the wide disparity between the two curves in Figure 5.

DISCUSSION

In this study, we have investigated the influence of a superposed tangential load on the evolution of subsurface radial cracks in convex glass surfaces on polymeric supports. The tangential load has been effected by loading the hemispherical glass surfaces vertically but off-axis, specifically at 30° to the symmetry axis. As with axial loading, radial cracks form directly under the indenter along the specimen surface normal at the glass undersurface. Critical loads $P = P_R$ to initiate the radial cracks are not significantly different at $\phi = 30^\circ$ than at $\phi = 0$ (Figure 4). Also, the radial crack patterns remain essentially symmetrical in their early stages of development (Figure 2). These two sets of observations, taken together, suggest little perturbation from the tangential load on the tensile hoop stress distribution at the glass layer undersurface. This conclusion is in accord with an earlier study on flat layer structures.⁵ On the other hand, as in the case of axial loading, the critical load P_R does increase monotonically, if slowly, with glass inner surface curvature (Figure 4).

The influence of tangential loading is felt much more strongly in the ensuing propagation stages of radial fracture. The cracks tend to depart from radial symmetry, and accelerate more rapidly toward the closest specimen edge (Figure 3). The loads P_F to take the specimens to failure at their support bases are substantially reduced, by about a factor of 2 for the load inclination $\phi = 30^\circ$ examined here (Figure 5). Again, P_F for off-axis loading diminishes monotonically with increasing surface curvature, as for axial loading (Figure 5). Part of the reason for the relatively low loads in the off-axis case is simply geometrical, namely that the cracks have less distance to travel to the near boundaries as inclination angle ϕ increases (Figure 1). Part is also because of asymmetric enhancement of the tensile hoop stress along s toward the specimen edge (Figures 6 and 7).

We have dealt only with convex brittle surfaces here. In relation to dental crowns, the geometry can be a convoluted mixture of convex and concave surface areas. In our preceding article, radial cracking was found to be severely inhibited in axial contacts on concave surfaces, and therefore of lesser interest in the context of failure.¹ Accordingly, we have not included concave surfaces in the present study. However, extended studies of more complex surface shapes containing both convex and concave surface areas, as befits typical crown structures, would appear to be an area worthy of investigation.

Further issues relating to the thickness of the ceramic crown, variations in elastic mismatch between the crown and substrate, configuration of the support base at the crown margins, cyclic loading, environmental effects, and flaw states, have been detailed in preceding papers.^{1,7} These are

additional items to be factored into the ultimate design of crown structures, and are left as issues for separate study.

From the dental context, the results suggest that crowns should be designed in such a way as to avoid areas of high convexity close to the margins in occlusal contact regions. More detailed studies of off-axis loading and convoluted curvatures would appear to be called for.

The authors gratefully acknowledge useful discussions with Matthew Rudas at the University of Western Australia, and Dianne Rekow and Van Thompson at New York University.

REFERENCES

1. Qasim T, Bush MB, Hu X, Lawn BR. Contact damage in brittle coating layers: influence of surface curvature. *J Biomed Mater Res* 2005;73B:179–185.
2. Chai H, Lawn BR, Wuttiphan S. Fracture modes in brittle coatings with large interlayer modulus mismatch. *J Mater Res* 1999;14:3805–3817.
3. Jung YG, Wuttiphan S, Peterson IM, Lawn BR. Damage modes in dental layer structures. *J Dent Res* 1999;78:887–897.
4. Lawn BR, Lee KS, Chai H, Pajares A, Kim DK, Wuttiphan S, Peterson IM, Hu X-Z. Damage-resistant brittle coatings. *Adv Eng Mater* 2000;2:745–748.
5. Lee C-S, Lawn BR, Kim DK. Effect of tangential loading on critical conditions for radial cracking in brittle coatings. *J Am Ceram Soc* 2001;84:2719–2721.
6. Lawn BR. Ceramic-based layer structures for biomechanical applications. *Current opinion in solid state and materials science* 2002;6:229–235.
7. Lawn BR, Deng Y, Miranda P, Pajares A, Chai H, Kim DK. Overview: damage in brittle layer structures from concentrated loads. *J Mater Res* 2002;17:3019–3036.
8. Deng Y, Lawn BR, Lloyd IK. Characterization of damage modes in dental ceramic bilayer structures. *J Biomed Mater Res* 2002;63B:137–145.
9. Zhao H, Miranda P, Lawn BR, Hu X. Cracking in ceramic/metal/polymer trilayer systems. *J Mater Res* 2002;17:1102–1111.
10. Lee C-S, Kim DK, Sanchez J, Miranda P, Pajares A, Lawn BR. Rate effects in critical loads for radial cracking in ceramic coatings. *J Am Ceram Soc* 2002;85:2019–2024.
11. Shrotriya P, Wang R, Katsube N, Seghi R, Soboyejo WO. Contact damage in model dental multilayers: an investigation of the influence of indenter size. *J Mater Sci Mater Med* 2003;14:17–26.
12. Lawn BR, Pajares A, Zhang Y, Deng Y, Polack M, Lloyd IK, Rekow ED, Thompson VP. Materials design in the performance of all-ceramic crowns. *Biomaterials* 2004;25:2885–2892.
13. Ford C, Bush MB, Hu XZ, Zhao H. A numerical study of fracture modes in contact damage in porcelain/Pd-alloy bilayers. *Mater Sci Eng* 2004;A364:202–206.
14. Wheeler RC. *A textbook of dental anatomy and physiology*. Philadelphia, PA: W. B. Saunders; 1958.
15. DeLong R, Douglas WH. Development of an artificial oral environment for the testing of dental restoratives: bi-axial force and movement control. *J Dent Res* 1983;62:32–36.
16. Phillips RW. *Skinner's science of dental materials*. Philadelphia: W. B. Saunders; 1991.
17. Kelly JR. *Ceramics in restorative and prosthetic dentistry*. *Ann Rev Mater Sci* 1997;27:443–468.
18. Kelly JR. Clinically relevant approach to failure testing of all-ceramic restorations. *J Prosthet Dent* 1999;81:652–661.
19. Malament KA, Socransky SS. Survival of Dicor glass-ceramic dental restorations over 14 years: I. Survival of Dicor complete

- coverage restorations and effect of internal surface acid etching, tooth position, gender and age. *J Prosthet Dent* 1999;81:23–32.
20. Malament KA, Socransky SS. Survival of Dicor glass-ceramic dental restorations over 14 years: II. Effect of thickness of Dicor material and design of tooth preparation. *J Prosthet Dent* 1999; 81:662–667.
 21. Malament KA, Socransky SS. Survival of Dicor glass-ceramic dental restorations over 16 years: Part III: effect of luting agent and tooth or tooth-substitute core structure. *J Prosthet Dent* 2001;86:511–519.
 22. Lawn BR, Deng Y, Thompson VP. Use of contact testing in the characterization and design of all-ceramic crown-like layer structures: a review. *J Prosthet Dent* 2001;86:495–510.
 23. Marshall DB, Lawn BR. Measurement of nonuniform distribution of residual stresses in tempered glass discs. *Glass Tech* 1978;19:57–58.
 24. Peterson IM, Pajares A, Lawn BR, Thompson VP, Rekow ED. Mechanical characterization of dental ceramics using hertzian contacts. *J Dent Res* 1998;77:589–602.
 25. Zhang Y, Lawn BR. Long-term strength of ceramics for biomedical applications. *J Biomed Mater Res* 2004;69B: 166–172.
 26. Ford C, Bush MB, Hu XZ, Zhao H. A numerical study of contact damage and stress phenomena in curved porcelain/glass-filled polymer bilayers. *Composites Sci Tech* 2004;64: 137–142.
 27. Ford C, Bush MB, Hu XZ, Zhao H. Numerical interpretation of cone crack initiation trends in a brittle coating on a compliant substrate. *Mater Sci Eng* 2004;A380:137–142.
 28. Kim H-W, Deng Y, Miranda P, Pajares A, Kim DK, Kim H-E, et al. Effect of flaw state on the strength of brittle coatings on soft substrates. *J Am Ceram Soc* 2001;84:2377–2384.